Electronic Spectrum of the AlC_2 Radical

Egor Chasovskikh, Evan B. Jochnowitz, Eunsook Kim, and John P. Maier*

Department of Chemistry, University of Basel, Klingelbergstrasse 80, CH-4056 Basel, Switzerland

Isabelle Navizet

Université Paris-Est, Laboratoire de Chimie Théorique, 5 bd Descartes, F-77454 Marne la Vallée cedex 2, France

Received: July 3, 2007; In Final Form: September 5, 2007

An electronic transition of the AlC_2 radical (C_{2v} structure) has been observed using laser-induced fluorescence spectroscopy. The molecule was prepared in a supersonic expansion by ablation of an aluminum rod in the presence of acetylene gas. A spectrum was recorded in the 451−453 nm region and assigned to the $\tilde{C}\,^2B_2-\tilde{X}\,^2A_1$ system ($T_0 = 22102.7$ cm^{-1}) based on a rotational analysis and agreement with calculated molecular parameters and excitation energies. Ab initio results obtained using couple cluster methods are in accord with previous theoretical work which concludes that ground-state AlC_2 possesses a T-shaped C_{2v} $^2A_1$ geometry, with the linear $^2\Sigma^+$ AlCC isomer 0.70 eV higher in energy. A fit of the experimental spectrum yields rotational constants in the ground and electronically excited states that are in reasonable agreement with the calculated values: $A'' = 1.7093(107)$, $B'' = 0.4052(50)$, $C'' = 0.3228(49)$ cm^{-1} for the $\tilde{X}\,^2A_1$ state, and $A' = 1.5621(137)$, $B' = 0.4028(46)$, $C' = 0.3201(54)$ cm^{-1} for $\tilde{C}\,^2B_2$. Variation in individual fluorescence lifetimes suggests that the emitting $\tilde{C}\,^2B_2$ state undergoes rovibronic mixing with lower lying electronic states.

Introduction

Metal carbides play an important role in the field of catalytic reactions, mainly due to the large surface areas that they tend to possess. Other recent advances in coating technologies have further fueled research in these compounds. Interest in gas-phase studies stems from the fact that smaller metal carbides are predicted to exist in space. While carbon is the most abundant heavy element in interstellar space, aluminum compounds containing halides, such as AlCl and AlF, as well as AlNC, have been detected in the inner circumstellar envelopes of carbon-rich stars through their rotational transitions.[1,2]

Dicarbides became a curiosity when both experiments and theory demonstrated that SiC_2 possesses a T-shaped geometry,[3,4] which was in direct conflict with the linear ground state structure of C_3.[5,6] Among theorists, there is general agreement that AlC_2 also has a T-shaped structure, with the C_{2v} conformation 33.5−46 kJ mol^{-1} more stable than the linear $C_{\infty v}$ geometry.[7−11] The high electron affinity of C_2 also suggests that stable dicarbides are likely formed with electropositive metals possessing low-ionization potentials, such as Al, Mg, or B.[12] Similarly, vibrational, rotational, and hyperfine structure in high-resolution spectra for the $\tilde{A}\,^2A_1$ - $\tilde{X}\,^2A_1$ transition of T-shaped YC_2 have also been analyzed.[13,14] Optical Stark measurements on the origin band led to the determination of a large dipole moment (6.38 D in the $\tilde{X}\,^2A_1$ state) confirming that the bonding in YC_2 is highly ionic.[15] Any structural parameters obtained from studying AlC_2 will help expand the understanding of more complex metal carbide systems. Spectroscopically determined constants offer a means to identify these molecules in interstellar environments.

Recent structural calculations found that the C_{2v} T-shaped structure is more stable than the linear $C_{\infty v}$ geometry by 47.66 kJ mol^{-1} using a single point QCISD(T) calculation (36.69 kJ mol^{-1} using DFT B3LYP).[10] The same study reports a 37.20 kJ mol^{-1} barrier (B3LYP) for isomerization from the T-shape to linear form, versus a 0.50 kJ mol^{-1} barrier for the reverse reaction, thus indicating that any linear $C_{\infty v}$ AlC_2 will be easily converted into the C_{2v} isomer.

Previous experimental work on the AlC_2 radical includes electron spin resonance studies in rare gas matrices.[16] Here, the T-shaped structure of AlC_2 was confirmed and led to the assignment of the $\tilde{X}\,^2A_1$ ground state. Bonding characteristics were also analyzed, indicating that the aluminum atom interacts with C_2 by donating electron density to the more electronegative C_2 through both $\sigma-$ and π-molecular orbitals.

Although AlC_2 has not yet been detected in the IR, theoretical methods have been used to calculate vibrational frequencies in the ground state: a single point QCISD optimization yielded the low-frequency b_2 mode (404.8 cm^{-1}) and the two a_1 vibrational modes (624.4 and 1761 cm^{-1}).[10] CASSCF theory with a VDZ basis set reports frequencies of 442, 680.2, and 1733.1 cm^{-1} for the same vibrations.[8]

The energy difference between the $\tilde{X}\,^2A_1$ and $\tilde{A}\,^2A_1$ states in neutral AlC_2 was determined as 0.98 eV through an analysis of the photoelectron spectrum of the AlC_2^- anion.[17] A vibrational progression was assigned to a 590 cm^{-1} Al−C_2 stretch in both the ground and excited $^2A_1$ states.

Rotational constants for the equilibrium structures of the T-shaped AlC_2 radical were calculated as: $A_e = 50.76$, $B_e = 12.00$, and $C_e = 9.705$ GHz.[7] A more recent study, using a B3LYP/6-311G(d) method, reports $A_e = 52.657$, $B_e = 11.814$, and $C_e = 9.650$ GHz for a similar T-shaped structure.[11]

Experimental Section

Jet-cooled AlC_2 was produced using laser vaporization (532 nm) of a pure aluminum rod in the flow of 5% acetylene in

* Corresponding author. E-mail: j.p.maier@unibas.ch. Phone: +41 61 267 38 26. Fax: +41 61 267 38 55.

10.1021/jp075169e CCC: $37.00
Published on Web 10/30/2007

TABLE 1: Optimized Geometry for $\tilde{X}\ ^2A_1$ (C_{2v}) AlC_2 and Calculated Vibrational Frequencies (cm^{-1})

	CCSD(T)	QCISD/6-311G* (ref 10)
r_{C-C}	1.276 Å	1.280 Å
r_{Al-C}	1.928 Å	1.937 Å
α_{C-Al-C}	38.7°	38.6°
ω_1 a_1	1735	1761
ω_2 a_1	645	624
ω_3 b_2	421	405

TABLE 2: Vertical Transition Energies (eV) for Excitations with Transition Moments Greater than 0.2 a.u., Calculated at the Minimum Geometry

transition	CASSCF	MRCI+Q	transition moment (a.u.)
$\tilde{A}\ ^2A_1 - \tilde{X}\ ^2A_1$	1.195	1.200	0.995 (*Z*)
$\tilde{F}\ ^2A_1 - \tilde{A}\ ^2A_1$	3.011		−0.470 (*Z*)
$\tilde{E}\ ^2B_2 - \tilde{C}\ ^2B_2$	0.809		0.394 (*Z*)
$\tilde{B}\ ^2B_1 - \tilde{A}\ ^2A_1$	1.024		−0.334 (*X*)
$\tilde{D}\ ^2B_1 - \tilde{X}\ ^2A_1$	2.947	3.271	0.335 (*X*)
$\tilde{D}\ ^2B_1 - \tilde{A}\ ^2A_1$	1.752		−0.230 (*X*)
$\tilde{C}\ ^2B_2 - \tilde{X}\ ^2A_1$	2.770	2.752	0.471 (*Y*)
$\tilde{E}\ ^2B_2 - \tilde{X}\ ^2A_1$	3.580	3.830	0.422 (*Y*)
$\tilde{E}\ ^2B_2 - \tilde{A}\ ^2A_1$	2.385		0.367 (*Y*)

helium or argon gas (10 bar) provided by a 0.3 mm orifice-pulsed valve. The rod was rotated and translated so that a fresh surface was continuously exposed to the laser, which was fired to coincide with the gas flow over the target area. The vaporization plume flows through a channel (3 mm diameter by 5 mm long) before undergoing a free-jet expansion.

The resulting AlC_2 radicals are then probed through laser-induced fluorescence (LIF) using an excimer-pumped dye laser (0.15 cm^{-1}) with a wavemeter used for frequency calibration. The fluorescence signal was collected by an *f*/1 lens and detected using a photomultiplier and a digital oscilloscope.

Results

Ab initio calculations using the MOLPRO program[18] with an aug-cc-pVQZ basis set of Dunning et al.[19,20] were carried out for the electronic states of AlC_2. The coupled cluster with perturbative triples (CCSD(T)) method was used for the description of the $\tilde{X}\ ^2A_1$ ground state. For comparison, the ground-state linear $^2\Sigma_g^+$ isomer AlCC was also calculated and found to lie 0.70 eV higher in energy. The optimized geometries for the electronic C_{2v} ground state and the harmonic frequencies of the fundamental vibrational transitions are compared with previous work in Table 1.[10]

The vertical transition energies for the lowest excited states whose transition moments are greater than 0.2 au are listed in Table 2 at the ground state equilibrium geometry. Full valence CASSCF calculations were performed with 8 states (3 a_1, 2 b_1, 2 b_2, 1 a_2, all in C_{2v} symmetry). Higher level calculations for vertical transitions originating from the $\tilde{X}\ ^2A_1$ state have also been performed at the MRCI level of theory with the results listed in Table 2. Finally, the excited $\tilde{C}\ ^2B_2$ state has been optimized at the MRCI level of theory in C_{2v} geometry. The minimum lies 2.684 eV above the $\tilde{X}\ ^2A_1$ ground state. The geometries calculated for the upper and lower states are shown in Figure 1.

The bottom trace in Figure 2 shows the experimental spectrum (0.15 cm^{-1} resolution) for the $\tilde{C}\ ^2B_2 - \tilde{X}\ ^2A_1$ transition of AlC_2. The signal was dependent on the presence of aluminum. The spectrum was not observed when acetylene was missing from the buffer gas mixture, indicating that carbon and/or hydrogen must be present in the spectral carrier. Substituting deuterated acetylene had no effect, thus eliminating the role of hydrogen.

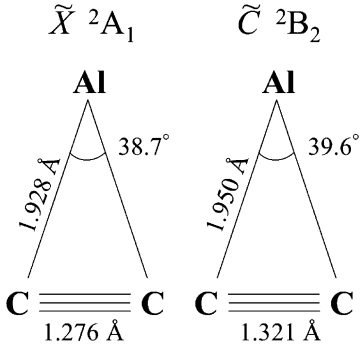

Figure 1. Optimized geometries for the AlC_2 radical calculated at the CASSCF level of theory.

The recorded spectrum was thus assigned to the $\tilde{C}\ ^2B_2 - \tilde{X}\ ^2A_1$ transition of AlC_2, one of the stronger transitions listed in Table 2, based on its observed frequency. Scanning to the red revealed no additional band systems, thereby allowing a confident assignment of the observed band as the origin of the $\tilde{C}\ ^2B_2 - \tilde{X}\ ^2A_1$ transition.

Decay curves were measured for 21 rotational peaks in the origin band of the $\tilde{C}\ ^2B_2 - \tilde{X}\ ^2A_1$ transition of AlC_2, in the range from 22 065 to 22 116 cm^{-1}. The decay curves appeared exponential and were found to vary from 140 to 640 ns. This substantial scatter is shown graphically in Figure 3 where the measured lifetimes are plotted above a portion of the experimental spectrum reproduced from Figure 2.

Discussion

A rotational analysis using the program "WANG" was performed with a conventional Hamiltonian for an asymmetric top assuming a *b*-type transition in a C_{2v} molecule.[21] In particular six Q-branch heads, which are associated with $\Delta K \pm 1$ sub-bands that result from the perpendicular nature of the transition, were used to guide the fit. These are labeled in Figure 2 using the notation $Q(K_a' - K_a'')$. In all, a selection of 14 lines, including P-branch lines from the $K_a' - K_a''$ (3−4) and $K_a' - K_a''$ (1−0) manifolds, was included in the least-squares optimization to obtain the best parameters for the rotational analysis. Any increase in the number of fitted lines tended to be detrimental to achieving a successful fit, presumably because of the substantial blending of lines due to the limited resolution achievable in measuring the experimental spectrum. The temperature used for modeling the spectrum was 70 K and the line width was fixed at 0.15 cm^{-1}. The resulting simulation is shown as the upper trace in Figure 2.

As with SiC_2,[3] the two carbon atoms in this molecule are equivalent and interchangeable through rotation around the "*a*"-inertial axis. In a near-prolate asymmetric top, equivalent zero spin nuclei that are symmetric with respect to rotation about the "*b*"-axis will produce alternation in the *J* structure. Here, in a C_{2v} geometry, the equivalent zero-spin nuclei are identical through 2-fold rotation about the *a*-axis, producing alternation in the *K* rotational structure (K_a). For AlC_2 the nuclear spin statistical weights of odd K_a'' levels ($K_a'' = 1, 3, ...$) are zero, hence there should be no evidence of any sub-bands originating from these states. Taking into account these alternation effects is essential for the fitted spectrum to more closely resemble the observed one, offering further verification of the spectral carrier.

However, as may be seen from the comparison shown in Figure 2, a perfect fit between the rotational analysis and the experimental spectrum was not achieved. This may be attributed to two factors. One possibility is that $\tilde{C}\ ^2B_2$ rovibronic levels

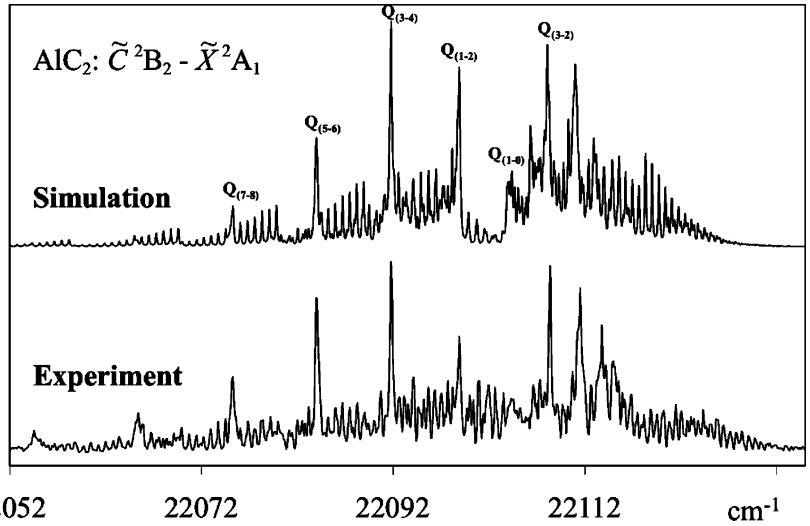

Figure 2. The origin band in the $\tilde{C}\,^2B_2 - \tilde{X}\,^2A_1$ electronic transition for AlC_2, recorded via laser-induced fluorescence. The lower trace is the experimental spectrum, while the upper trace depicts the simulated fit. Q-branch heads that are associated with $\Delta K \pm 1$ sub-bands and were used to guide the spectral fit are labeled $Q(K_a' - K_a'')$.

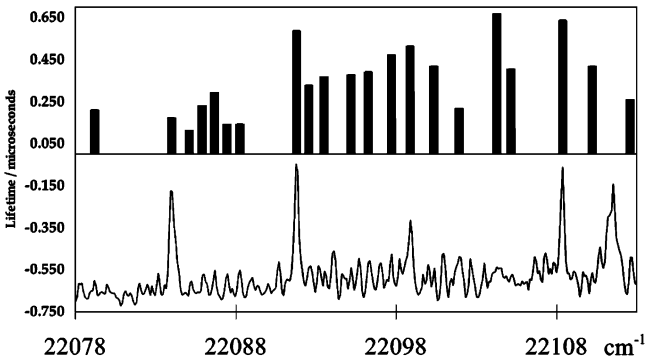

Figure 3. The origin band in the $\tilde{C}\,^2B_2 - \tilde{X}\,^2A_1$ electronic transition for AlC_2, reproduced from Figure 2. Above the spectrum lie depictions of the fluorescent lifetimes measured.

are perturbed as a result of rovibronic coupling with levels associated with lower lying electronic states. These can include near-degenerate b_2 levels of the $\tilde{A}\,^2A_1$ and $\tilde{X}\,^2A_1$ states or lower lying quartet states that have not yet been located. Through vibronic and Coriolis operators A_1, A_2, and B_1 states may also interact in a rotational-dependent manner, thus perhaps also perturbing the observed system.

The lifetimes of various lines in the spectrum were measured in an effort to qualitatively examine the extent of mixing among the electronic states in AlC_2, giving rise to the wide variation in τ depicted in Figure 3. In an earlier study on the $\tilde{A}\,^1B_1 - \tilde{X}\,^1A_1$ transition of SiH_2 (C_{2v}), wide variations in the fluorescent lifetimes of individual rotational lines (few nanoseconds to >1 μs) were attributed to rovibronic perturbations.[22,23] Specifically, rovibronic levels in the SiH_2 $\tilde{A}\,^1B_1$ state mix with background levels from either the lower lying $\tilde{a}\,^3B_1$ state or highly excited vibrational levels from the $\tilde{X}\,^1A_1$ ground state, leading to perturbations in the energy levels and oscillator strengths and thus making a spectral fit impossible using a standard rotational Hamiltonian. Similar behavior has also been reported for the fluorescence decay rates found in the S_1 ($\tilde{A}^1A_2$) states of formaldehyde.[24,25]

This mixing can be sensitive to rotational quantum number[26] and the proximity and identity of near degenerate background states, leading to seemingly random perturbations in oscillator strengths and energy level positions and thereby influencing the experimental measurement of the rotational contour. Figure 3 shows that some Q-branch band maxima associated with the $\Delta K \pm 1$ sub-bands possess lifetimes up to 2−3 times longer than other lines. These longer lifetimes may arise due to quartet dilution, whereby a substantial fraction of spin forbidden quartet character is added to the emitting $\tilde{C}\,^2B_2$ state. Conversely, other high J-levels demonstrate shortened lifetimes, which may be due to a stronger coupling with b_2 vibronic states from the $\tilde{A}\,^2A_1$ and $\tilde{X}\,^2A_1$ electronic states, resulting in increased nonradiative decay rates.

A second reason for the imperfect fit to the experimentally observed spectrum may derive from a non-Boltzmann temperature distribution in the jet: that is, in an expanding jet the J-levels cool more efficiently than the K-levels. This has been previously observed in beams of glyoxal[27] and acetaldehyde[28] that were also studied using LIF. In the case of acetaldehyde, the rotational temperature for molecules in the beam was found to be over four times higher in K-quantum number than in J. This same effect is apparent in the spectral simulation of AlC_2, where at 70 K the J-temperature seems to fit reasonably well; however, the intensity distribution in the Q-branch heads appears to fall faster than in the experimental spectrum. This would seem to indicate that to correctly simulate the spectrum one would have to model an increased K-temperature while holding the J-temperature at its current value. This has not been carried out at this stage because a reasonable fit was obtained yielding rotational constants consistent with the theoretical structures calculated for the $\tilde{X}\,^2A_1$ and $\tilde{C}\,^2B_2$ states.

The molecular constants obtained are given in Table 3, along with the corresponding MRCI calculated values. Conservative errors were qualitatively estimated through fixing the resulting constants and then systematically varying each parameter. In general, constants could be varied by approximately twice the value of the standard deviations derived from the spectral fitting procedure before the modeled spectrum significantly differed from the experimentally obtained one. Error in T_0 stems from the spectral line width used to measure the transition.

Geometric structures can be estimated from the rotational constants derived in the spectroscopic fit, with the C−C bond length calculated directly from the A constants. This yields r_{Al-C} and r_{C-C} as 1.93 and 1.28 Å for the $\tilde{X}\,^2A_1$ ground state, and 1.94 and 1.34 Å for the excited $\tilde{C}\,^2B_2$ state. All values are within error of the calculated CASSCF geometries shown in Figure 1.

TABLE 3: Rotational Constants (cm^{-1}) Obtained from a Geometry Optimization Performed at the MRCI Level of Theory and from the Rotational Analysis[a]

	MRCI	spectral fit
	$\tilde{X}\,^2A_1$	
A″	1.725 cm^{-1}	1.7093(107) cm^{-1}
B″	0.400 cm^{-1}	0.4052(50) cm^{-1}
C″	0.325 cm^{-1}	0.3228(49) cm^{-1}
	$\tilde{C}\,^2B_2$	
A′	1.609 cm^{-1}	1.5621(137) cm^{-1}
B′	0.394 cm^{-1}	0.4028(46) cm^{-1}
C′	0.316 cm^{-1}	0.3201(54) cm^{-1}
T_0		22102.7 ± 0.2 cm^{-1}

[a] Errors in the rotational constants represent twice the standard deviations derived from the fit.

Conclusion

The electronic spectrum of AlC_2 was observed using an ablation source and laser induced fluorescence detection. The experiments demonstrated that the spectral carrier contained only Al and C atoms. The rotationally resolved spectrum was assigned to the origin band of the $\tilde{C}\,^2B_2-\tilde{X}\,^2A_1$ system, a species that exists in a planar C_{2v} geometry as previously calculated. A rotational analysis is consistent with the asymmetric top AlC_2 (C_{2v}), further evidenced by the fact that nuclear spin effects due to two equivalent carbon atoms must be considered to properly model the experimental spectrum.

Molecular constants were estimated using a spectral simulation based on a least-squares fit to 14 individual lines. Spectroscopic constants obtained from the fit compare reasonably well with ab inito calculations performed on both the ground and excited states. The imperfect nature of the fit is attributed to an inability to account for substantial interactions with lower lying quartet and $^2A_1$ states that manifest themselves as irregular perturbations in both the energy levels and their oscillator strengths. Being able to incorporate a non-Boltzmann temperature dependence for the *J*- and *K*-levels may also enable a more accurate fit. However, as it stands, the fit confirms the perpendicular nature of the $\tilde{C}\,^2B_2-\tilde{X}\,^2A_1$ transition.

Finally, further confirmation of the carrier's identity was obtained using a resonant 2-color 2-photon ionization technique, where a spectrum of AlC_2 was observed in the same 452 nm region for the *m*/*z* 51 mass.[29] A more detailed analysis awaits the collection of a higher resolution spectrum.

No matches corresponding to the diffuse interstellar band literature were found for the origin band of AlC_2; however, the information obtained in this study can aid further attempts to identify this dicarbide species in interstellar space by means of its electronic spectrum. The spectroscopic constants also offer a guide for future microwave investigations.

Acknowledgment. We thank Professor Alan E. W. Knight for helpful discussions. This work has been supported by the Swiss National Science Foundation (Grant 200020-115864/1) and the European Office of Aerospace Research and Development (Grant FA8655-07-1-30310).

References and Notes

(1) Cernicharo, J.; Guélin, M. *Astron. Astrophys.* **1987**, *183*, L10.
(2) Ziurys, L. M.; Savage, C.; Highberger, J. L.; Apponi, A. J.; Guélin, M.; Cernicharo, J. *Astrophys. J.* **2002**, *564*, L45.
(3) Michalopoulos, D. L.; Geusic, M. E.; Langridge-Smith, P. R. R.; Smalley, R. E. *J. Chem. Phys.* **1984**, *80*, 3556.
(4) Grev, R. S.; Schaefer, H. F. *J. Chem. Phys.* **1984**, *80*, 3552.
(5) Douglas, A. E. *Astrophys. J.* **1951**, *114*, 466.
(6) Clusius, K.; Douglas, A. E. *Can. J. Phys.* **1954**, *32*, 319.
(7) Flores, J. R.; Largo, A. *Chem. Phys.* **1990**, *140*, 19.
(8) Chertihin, G. V.; Andrews, L.; Taylor, P. R. *J. Am. Chem. Soc.* **1994**, *116*, 3513.
(9) Yang, H.; Tanaka, K.; Shinada, M. *THEOCHEM-J. Mol. Struct.* **1998**, *422*, 159.
(10) Zheng, X.; Wang, Z.; Tang, A. *J. Phys. Chem. A* ***1999***, *103*, *9275*.
(11) Redondo, P.; Barrientos, C.; Largo, A. *Int. J. Quantum Chem.* **2004**, *96*, 615.
(12) Green, S. *Chem. Phys. Lett.* **1984**, *112*, 29.
(13) Steimle, T. C.; Marr, A. J.; Xin, J.; Merer, A. J.; Athanassenas, K.; Gillet, D. *J. Chem. Phys.* **1997**, *106*, 2060.
(14) Steimle, T. C.; Bousquet, R. R.; Namiki, K. C.; Merer, A. J. *J. Mol. Spectrosc.* **2002**, *215*, 10.
(15) Bousquet, R. R.; Steimle, T. C. *J. Chem. Phys.* **2001**, *114*, 1306.
(16) Knight, L. B.; Cobranchi, S. T.; Herlong, J. O.; Arrington, C. A. *J. Chem. Phys.* **1990**, *92*, 5856.
(17) Boldyrev, A. I.; Simons, J.; Li, X.; Wang, L.-S. *J. Am. Chem. Soc.* **1999**, *121*, 10193.
(18) Werner, J.-J.; Knowles, P. J. MOLPRO; http://www.molpro.net.
(19) Dunning, T. H. *J. Chem. Phys.* **1989**, *90*, 1007.
(20) Kendall, R. A.; Dunning, T. H.; Harrison, R. J. *J. Chem. Phys.* **1992**, *96*, 6796.
(21) Luckhaus, D.; Quack, M. *Mol. Phys.* **1989**, *68*, 745.
(22) Thoman, J. W.; Steinfeld, J. I.; McKay, R. I.; Knight, A. E. W. *J. Chem. Phys.* **1987**, *86*, 5909.
(23) McKay, R. I.; Uichanco, A. S.; Bradley, A. J.; Holdsworth, J. R.; Francisco, J. S.; Steinfeld, J. I.; Knight, A. E. W. *J. Chem. Phys.* **1991**, *95*, 1688.
(24) Weisshaar, J. C.; Moore, C. B. *J. Chem. Phys.* **1980**, *72*, 5415.
(25) Guyer, D. R.; Polik, W. F.; Moore, C. B. *J. Chem. Phys.* **1986**, *84*, 6519.
(26) Knight, A. E. W. Rotational Involvement in Intramolecular Vibrational Redistribution. In *Excited States*; Lim, E. C., Ed.; Academic Press: New York, 1988; Vol. 7.
(27) Peyroula, E. P.; Jost, R. *J. Mol. Spectrosc.* **1987**, *121*, 167.
(28) Price, J. M.; Mack, J. A.; von Helden, G.; Yang, X.; Wodtke, A. M. *J. Phys. Chem.* **1994**, *98*, 1791.
(29) Apetrei, C.; Chasovskikh, E.; Ding, H.; Jochnowitz, E. B.; Maier, J. P. In preparation.